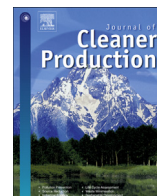




Contents lists available at ScienceDirect

Journal of Cleaner Production

journal homepage: www.elsevier.com/locate/jclepro

Phosphorus immobilization by the surface sediments under the capping with new calcium peroxide material

Jing Zhou, Dapeng Li^{*}, Zhehao Zhao, Xiaojun Song, Yong Huang, JingJing Yang

School of Environmental Science and Engineering, Suzhou University of Science and Technology, No.1, Kerui Road, Suzhou, 215009, China

ARTICLE INFO

Article history:

Received 5 July 2019

Received in revised form

30 September 2019

Accepted 1 November 2019

Available online xxx

Handling editor: M.T. Moreira

Keywords:

Calcium peroxide

Remediation

Adsorption

Phosphorus fractions

Surface sediment

ABSTRACT

Capping material plays an important role in P (phosphorus) control. However, P immobilization on surface sediments due to the remediation by the capping materials has been neglected. Herein, we conducted an experiment to research the mechanism of surface sediment on P immobilization under new calcium peroxide material (NCPM) capping at different ratios of the sedimentary mobile phosphorus (P_{mobile} , the sum of $\text{NH}_4\text{Cl-P}$, BD-P and NaOH-nrP) to NCPM (1:1–1:4). The concentrations of soluble reactive P (SRP), ammonium (NH_4^+) and ferrous (Fe(II)) in water and sedimentary P fractions were analyzed. The study also presents the results of Langmuir isotherm model for surface sediments and sedimentary P release under anaerobic conditions. The results show that the surface sediments under NCPM capping improved the SRP reduction both from overlying and pore water. This was attributed to Ca^{2+} precipitation and sedimentary micro-environment change from anaerobic conditions to aerobic conditions which resulted from the NH_4^+ and Fe(II) concentration reductions. This remediation increased maximum adsorption capacity (S_{max}) and decreased equilibrium concentration of P adsorption and desorption (EPC_0) in those surface sediments under NCPM capping, which was favourable for P adsorption and immobilization. The X-ray diffraction and energy-dispersive X-ray spectroscopy analyses results confirmed aforementioned results. The conversion of P fractions from P_{mobile} to inert P in the surface sediments was more obvious than control. The inert P increased from 50.15% (1:1) to 69.88% (1:4), resulting in lower P release from the surface sediments under NCPM capping, compared with the control. The results show that NCPM capping improved P removal and immobilization of the surface sediments, beneficial for controlling sedimentary P release.

© 2019 Elsevier Ltd. All rights reserved.

1. Introduction

Phosphorus (P) has long been identified as a vital limiting element in lake eutrophication, which has become a global environmental problem, inducing a series of threats, including frequent algal blooms, hypoxia and black-odor problems (Stow and Cha, 2013). Even though external P has been controlled recently, the internal P was still released from sediments into water, hindering the restoration of water quality (Yu et al., 2017; Wang et al., 2017;

Yin and Kong, 2015). Therefore, minimizing release of sediment-bound P to water is a key factor in preventing lake eutrophication.

Different technologies have recently been developed to inhibit the P release from sediment (Sibrell et al., 2009; Francingues et al., 2008; Pan et al., 2012). An increasing number of researchers are focusing on in-situ capping to inhibit internal P release. For example, Ca-based compounds have been widely used as capping materials to inhibit sedimentary P releasing because of convenience of implementation, low cost and environmental compatibility. Wang et al. (2018a,b) investigated Ca-decorated biochar (Ca-BC) with a maximum P adsorption ability of 314.22 mg g^{-1} when the Ca/BC mass ratio was 2:1. Yin and Kong (2015) reported that natural Ca-rich attapulgite (NCAP700) effectively bound 34.5% of Sediment-mobile P (P_{mobile}) in lake sediments via thin-layer capping. Li et al. (2017) investigated that 90% P was prevented to release from sediments into water when capped with calcium silicate hydrates. In addition, the concentration of Ca-P and exchangeable-P in the sediments increased.

Abbreviations: P, phosphorus; SRP, soluble reactive phosphorus; TP, total phosphorus; NCPM, new calcium peroxide material; Tot-P, total phosphorus in sediments; BD-P, Fe-bound P; Al-P, Al-bound P; Ca-P, Ca-bound P; Res-P, residual phosphorus; Fe, iron; Al, aluminum; Ca, calcium; Fe(II), ferrous; Fe(III), ferric; NH_4^+ , ammonium; q_{max} , maximum adsorption capacity; EPC_0 , equilibrium concentration of P adsorption and desorption.

^{*} Corresponding author.

E-mail address: ustslp@163.com (D. Li).

<https://doi.org/10.1016/j.jclepro.2019.119135>

0959-6526/© 2019 Elsevier Ltd. All rights reserved.

Other studies (Yamada-Ferraz et al., 2015; Meis et al., 2013; Wang et al., 2019) have shown that adsorption capacity and immobilization ability of the capping materials play the most important role in controlling sedimentary P release. However, few investigations have focused on the remediation of surface sediments by the capping materials to improve P inhibition capacity. Generally, the remediation of the surface sediments leads to a change of the microenvironment in the surface sediments from aerobic conditions to anaerobic conditions. In anaerobic condition, insoluble oxidized Fe(III) oxides and hydroxides which possess strong phosphate bound capability, trend to reduce to Fe(II) oxides and hydroxides, and result in the sedimentary P release (Ding et al., 2018; Li et al., 2017). Correspondingly, these anaerobic microenvironment conditions of sediment could cut down the ability of capping materials to inhibit the release of P from sediment (Meis et al., 2012). Therefore, a better capping material with the ability to not only adsorb and immobilize P but also remold the surface sediments to provide long-term P retention is needed.

CaO₂ is a promising material that may solve many environmental problems (Huang et al., 2019) and satisfy the aforementioned requirements. However, due to its quick release of oxygen, ability to increase the pH and the physical barrier formed when reacting with water which induce the weak permeability of O₂ to sediments, CaO₂ has not been widely used as a capping material (Fox and Tuchman, 1996). Therefore, increasingly modifications based on the combination with other substances to retard the release rate of CaO₂, H₂O₂ and O₂ were developed. Zhou et al. (2019) found that when the mixing ratio of CaO₂: water purification sludge: cement blend was 5:3:2 and made into pies extended the supplement of oxygen and promoted the transformation of immobilized P. These previous studies suggest that CaO₂ mixed with water purification sludge and cement is a better choice for retarding the quick release of oxygen. However, less information is available about the change of the sedimentary microenvironment in the surface sediments under the capping of the materials with oxygen supply and its effects on the adsorption and immobilization of sedimentary P.

Compared with other oxygen generators (Ashley et al., 2008; Müller and Stadelmann, 2010), CaO₂ has another distinctive property in its ability to supplement Ca, which binds P by precipitation, thereby promoting the transformation of P_{mobile} to inert-P by enhancing the sedimentary P immobilization capacity (Hanh et al., 2005). CaO₂ can enhance the sedimentary P retention ability of surface sediments because of the precipitation of Ca, the change of microenvironment by CaO₂ oxidation.

This study aims to investigate P immobilization under different dosages of CaO₂ as a form of new calcium peroxide material (NCPM). The object of this study was: (1) to investigate the effect of the NCPM on the P in overlying water and the SRP (soluble reactive phosphorus) concentration in pore water; (2) to characterize the change of the sedimentary micro-environment in the surface sediment, which is described by the variations in Fe(II) (Ferrous) and NH₄⁺ (Ammonium), the P adsorption by the adsorption isotherm, and the P release under the anaerobic conditions; (3) to assess the transformation of P fractions due to the integrated influence of the oxygen and Ca.

2. Materials and methods

2.1. Site description, sample collection and materials preparation

NCPM were produced by blending CaO₂ (calcium peroxide), WPS (water purification sludge) with cement in the ratio of 5:3:2 according to previous study (Zhou et al., 2019). NCPM were insoluble solid particles with 0.5 cm diameter and used for capping.

Additional characteristic about NCPM reported in Zhou et al. (2019).

The water and sediments samples were collected from the canal (N31°16'23.86", E120°37'50.43") which located in Suzhou of China with the average depth of 2.5 m. The canal is a typical eutrophic canal due to the pollution input. Sediments were taken by the piston sampler (Rigo Co., 84 mm i.d., 500 mm long) and transported to the lab directly, put sediments through #100 aperture sieve and stored at 4 °C in the dark. A 75-L water simple at the sediment sampling point was sampled. The characteristic of water and sediment samples are listed in Table 1.

2.2. External P removal experiment

Five sets of Plexiglas tubes (i.d. 84 mm, height 200 mm) with 15 cm height of wet sediment were used for the experiment, and each set contained three parallel samples. The control was prepared with only sediment. In term of samples E1, E2, E3 and E4, the ratio of sedimentary P_{mobile} to NCPM was 1:1 (1.84 g), 1:2 (3.68 g), 1:3 (5.51 g) and 1:4 (7.35 g), respectively. Overlying water (300 mL) from sample point was siphoned into water to avoid sediments disturbance. After equilibrium, Rhizon samplers were set into preformed holes at depths of 1 cm, 2 cm, 3 cm and 5 cm under the sediment–water interface to collect pore water.

These cylinders were sampled at room temperature. The collection of 3 mL overlying water was at 2-day intervals measured of the concentration of SRP. 3 mL of 30 mg P L⁻¹ anhydrous KH₂PO₄ solution was added to each cube after measurement for the simulation of external P input until the saturation of adsorption. 5 mL pore water were collected by Rhizon samplers for measuring concentration of SRP, NH₄⁺ and Fe(II) at 3-day intervals and raw water from a lake was added for supplement. This experiment was last for 60 days.

At the end of experiment, Sediments were collected at different depths after overlying water siphoned out. These sediments were sieved through the #100-mesh sieve after dry and stored in airtight flasks for analysis.

2.3. Batch isothermal adsorption by the surface sediments

To evaluate P adsorption capacity of surface sediments due to the addition of NCPM, isothermal adsorption batch experiment was set. After the external P removal experiment was finished, the surface sediments without NCPM were taken and used for the batch isothermal adsorption experiment. 0.5 g homogenized and dry sediment was placed in 50 mL different the initial P concentrations (anhydrous KH₂PO₄): 0, 0.05, 0.1, 0.2, 0.5, 1.0, 2.0, 4.0, 10.0, 20.0, 50.0 and 80.0 mg P L⁻¹. Sediment to liquid was at the ratio of 1:100. After mixing 30 min, the pH in the overlying water were 5.95 (control), 6.09 (1:1), 6.20 (1:2), 6.31 (1:3), 6.49 (1:4), respectively.

Adsorption experiments performed to equilibrium (200 r min⁻¹, 24 h, 25 ± 1 °C) and centrifuged (3500 r min⁻¹, 10 min) and filtered through a 0.45 μm cellulose acetate membrane and measured P concentrations. The P adsorption capacity of surface sediments were expressed as the difference between the P concentration of initial and final and used the Eq. (1) (Jin et al., 2005) as follow. The Langmuir model were adopted to fit the experimental data.

$$S = \left[\frac{S_{\max} \cdot n \cdot EPC}{1 + n \cdot EPC} \right] - S_0 \quad (1)$$

where S (mg kg⁻¹), S_{max} (mg kg⁻¹) and S₀ (mg kg⁻¹) represent the P adsorbed by the sediment, maximum P adsorption and P adsorbed under ambient conditions; EPC (mg L⁻¹) represents equilibrium solution P concentration; n represents the constant related to the bonding energy of P.

Table 1
Properties of water and sediment samples from canal.

Water					Sediment		
DO	pH	TP	SRP	NH ₄ ⁺ -N	Water content	LOI	Tot-P
mg·L ⁻¹		mg·L ⁻¹	mg·L ⁻¹	mg·L ⁻¹	%	%	g·kg ⁻¹
2.12	7.27	0.48	0.23	2.16	68.30	25.10	2074.81

EPC₀, the P concentration at the time of equilibrium without release or adsorption and calculated by Eq. (2):

$$EPC_0 = \frac{S_0}{n \cdot S_{\max} - n \cdot S_0} \quad (2)$$

2.4. P release from the surface sediments

To examine the P immobilization by the surface sediments due to the addition of NCPM, we conducted lab experiments of P release from the surface sediments which came from the external P removal experiment according to Abu-Hmeidan et al. (2018), keep the experiment proceeding with anaerobic conditions. Surface sediment samples were placed in a Ziploc bag after pre-treatment (Ziploc bags were placed in 1 mmol/L EDTA and boiled to remove the metal ions during production). The 10 mL distilled water was then added to one Ziploc bag and it was sealed with clips. Each bag was placed into a 250-mL conical flask which contains 250 mL of distilled water. The 200 mL distilled water was aerated with nitrogen for 20 min to ensure anaerobic conditions and then the flask was sealed using the lid to avoid of the air penetration into the flask. At last, these flasks were put into the dark. During the experiments, the lab temperature kept at about 20 °C. The aim was to promote and force the sedimentary P release into the overlying water. The 10 mL distilled water in the flask was taken for the measurement of SRP at the 12 h intervals and then the same volume of distilled water was replenished into the flask. The experiment was run for 7 days.

2.5. Sample analysis

SRP, NH₄⁺-N and Fe(II) concentrations were measured by the molybdenum blue method, the indophenol blue method, O-Phenanthroline spectrophotometric method, respectively (SEPA, 2002). Sediment P fractions measured in this study using the method exploited by Rydin (2000), where P fractions were divided into six types (Rydin, 2000), and using the sequential extraction method. NH₄Cl-P was extracted by 1M NH₄Cl for 2 h; BD-P was extracted by 0.11M Na₂S₂O₄/NaHCO₃ for 1 h; Al-P was extracted by 0.1M NaOH for 16 h; non-reactive P (NaOH-nrP) was calculated by NaOH-Tot P (The P concentration of the last step supernate after centrifugation and oscillation) minus Al-P; Ca-P was extracted by 0.5M HCl for 17 h; and residual P(Res-P) was extracted by 1.0M HCl for 16 h after 5 h ignition. The Tot-P is the sum of these P fractions. The P_{mobile} concentrations in sediment were calculated as the sum of NH₄Cl-P, BD-P, and NaOH-nrP (Lin et al., 2017).

2.6. Data analysis

One-way analysis of variance (ANOVA) was used to determine the difference of different NCPM dosages with respect of SRP, NH₄⁺, and Fe(II) in overlying water and pore water and NH₄Cl-P, BD-P, Al-P, NaOH-nrP, Ca-P, Res-P in sediment, p < 0.05 is considered significant. Statistical analyses were performed by employing

Statistical Production and Service Solution.

3. Results

3.1. SRP in overlying and pore water

Changes of concentration of SRP in overlying water with different dosages NCPM capping show in Fig. 1. For the control, the SRP concentration increased sharply to 1.65 mg P L⁻¹ with the addition of external P and then decreased gently when the external P addition was stopped (day 25). With NCPM capping, the SRP in overlying water gently increased to 0.81 mg P L⁻¹ (1:1), 0.69 mg P L⁻¹ (1:2), 0.48 mg P L⁻¹ (1:3) and 0.38 mg P L⁻¹ (1:4) (P < 0.01). The SRP concentration remained higher in the control than under the capping. Clearly, more addition of NCPM led to greater SRP removal. We calculated that the amount of P which disappeared from overlying water under NCPM capping was higher (3.97 mg (1:1), 5.15 mg (1:2), 6.97 mg (1:3) and 8.36 mg (1:4)) than the amount that disappeared from the control (2.29 mg) (P < 0.05).

Notably, the disappearance of external P was attributed to adsorption by NCPM or by the surface sediments. However, the storage of pore water cannot be neglected. Fig. 2 shows that the SRP concentration in pore water kept at a high-value level in the control than NCPM. Additionally, the concentration of SRP in pore water increased with increasing sediment depth. Under the NCPM capping, the concentration of SRP kept at a low-value level in the upper layer (0–1 cm and 1–2 cm) than in the deeper layer (2–3 cm and 4–5 cm). In the upper layer, the dosage of the NCPM strongly affected the SRP distribution in pore water. The average concentration of the SRP was 1.28 mg P L⁻¹ (Control), 0.39 mg P L⁻¹ (1:1), 0.47 mg P L⁻¹ (1:2), 0.29 mg P L⁻¹ (1:3) and 0.16 mg P L⁻¹ (1:4) in the sediment depth of 0–2 cm, respectively (P < 0.01). By contrast,

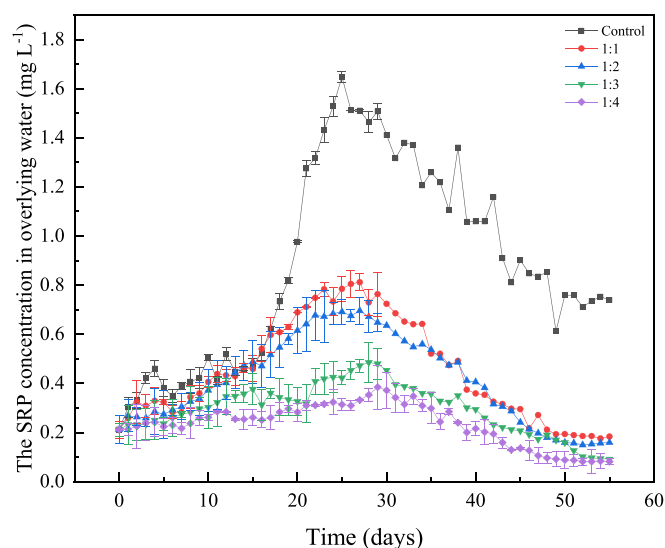


Fig. 1. SRP concentrations in the overlying water under the capping with NCPM. Bars indicate SEMs (n = 3).

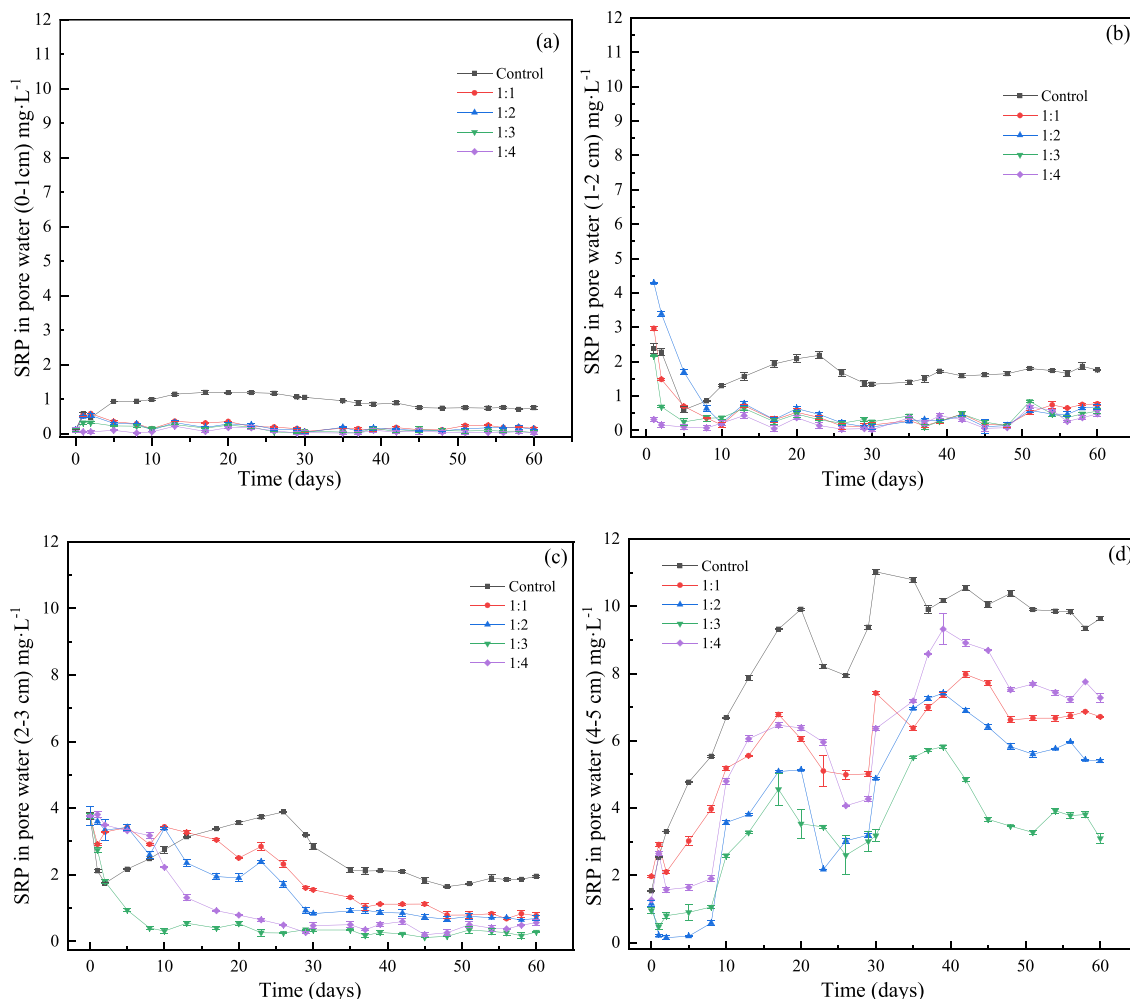


Fig. 2. SRP concentration of the pore water under the capping with NCPM. Bars indicate SEMs (n = 3).

in the deeper layer (4–5 cm), the SRP increased gradually and the peak value was 0.58 mg P L^{-1} (1:4). This result is likely closely related to the distribution of Fe(II) showed in Fig. 3.

3.2. Fe(II) and NH_4^+ in pore water

Fe(II), as the representative ion of anaerobic conditions, is the key reducing ion (Wang et al., 2019). The distribution of Fe(II) under the capping with the NCPM is shown in Fig. 3. Clearly, the concentration of Fe(II) was higher in the control than NCPM. The Fe(II) concentration in the control remained stable at different depths. By contrast, the Fe(II) concentration under the capping gradually decreased in the upper layer (0–1 cm and 1–2 cm) and the Fe(II) concentration decreased with increasing NCPM dosage. In the deeper (2–3 cm and 4–5 cm), the Fe(II) concentration showed the same trend as in the upper layer; However, the Fe(II) concentration was higher under the ratio of 1:4 than under the other ratios (1:1, 1:2, 1:3) ($P < 0.01$). This result is similar as the higher SRP concentrations in the pore water under the ratio of 1:4 in Fig. 2.

NH_4^+ is another reducing ion associated with anaerobic conditions (Kang et al., 2018). The NH_4^+ concentration (Fig. 4) showed a similar trend as the Fe(II) concentration (Fig. 3). During the experiment, the concentrations of the NH_4^+ at different depths in the control remained higher than under the NCPM capping. Under capping with NCPM, the average of NH_4^+ concentration was

4.99 mg L^{-1} (1:1), 5.34 mg L^{-1} (1:2), 4.85 mg L^{-1} (1:3) and 3.93 mg L^{-1} (1:4) in the depth of 0–1 cm ($P < 0.05$). The corresponding average increased to 24.27 mg L^{-1} (1:1), 22.53 mg L^{-1} (1:2), 18.30 mg L^{-1} (1:3) and 16.54 mg L^{-1} (1:4) at depths of 1–2 cm ($P < 0.05$). In the deeper layers (2–3 cm and 4–5 cm), the concentration of NH_4^+ was higher than that upper layers (0–1 cm and 1–2 cm). These results suggest that the microenvironment in the sediments trend to aerobic because of the oxygen release from the NCPM. In addition, the oxidation of the microenvironment in the sediments was better under the capping than control.

3.3. Changes of P fractions in sediments

The addition of external P caused a change in the sedimentary P fractions (Fig. 5). Under the ratio of 1:4, the Ca–P fraction was dominant, up to 32.22% (mean, 0–4 cm); the Al–P fraction was the second-most abundant, 21.90% (mean, 0–4 cm). Under the ratio of 1:3, Ca–P and Al–P were approximately equally dominant (~24%). Under the ratio of 1:2, Al–P was dominant, with a fraction as high as 27.55% (mean, 0–4 cm), and Ca–P was second-most abundant at 19.41% (mean, 0–4 cm). Under the ratio of 1:1, Al–P was dominant, as high as 27.37% (mean, 0–4 cm), $\text{NH}_4\text{Cl-P}$ was second-most abundant, 20.09% (mean, 0–4 cm). When compared with the control, the percentages of BD–P remained stable, whereas the percentage of Ca–P increased and that of NaOH–nrP clearly decreased

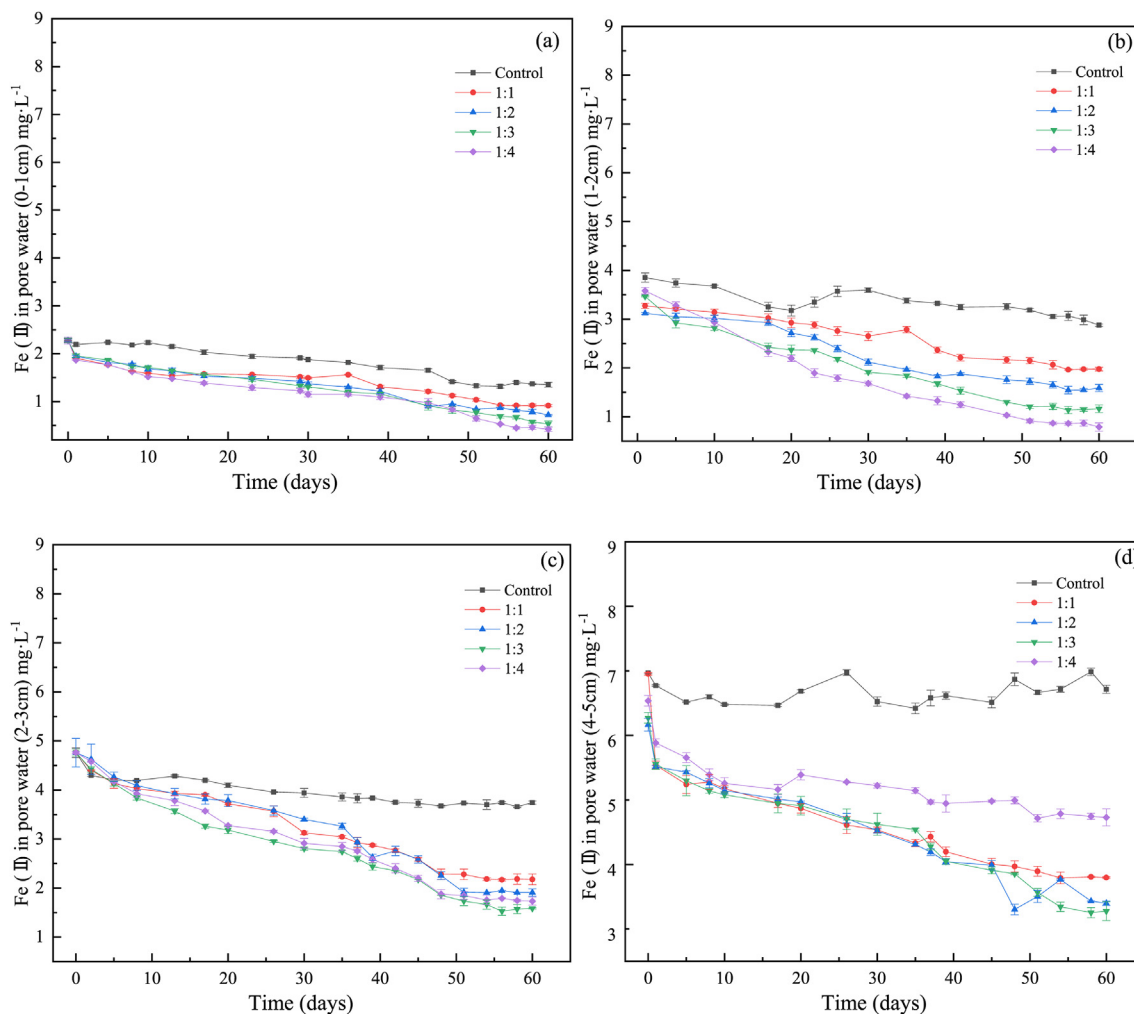


Fig. 3. Fe(II) concentration of the pore water under the capping with NCPM. Bars indicate SEMs (n = 3).

($P < 0.05$).

Fig. 5 shows that the percentages of $\text{NH}_4\text{Cl-P}$ and BD-P slightly declined with increasing NCPM dosage at same sediment depth, whereas the NaOH-nrP percentage decreased sharply. For NaOH-nrP , percentage decreases of 19.7% (0–1 cm) and 14.9% (1–2 cm) under the ratio of 1:4 were observed compared with the percentages under a ratio of 1:1. Contrarily, the percentages of Ca-P and Res-P increased with incremental NCPM at the same sediment depth. Ca-P in 0–1 cm increased from 22.1% under a ratio of 1:1–44.0% under a ratio of 1:4 ($P < 0.05$). Furthermore, the Al-P percentage remained stable under the different dosages of NCPM at the same sediment depth.

3.4. P adsorption isotherms of surface sediments

The adsorption of P by the surface sediments (in the experiments involving external P removal and immobilization after 60 days) under the addition of NCPM was investigated via P adsorption isotherm experiments (Fig. 6). The results in Fig. 6 suggest that the P adsorption abilities of surface sediments increased markedly under the capping with NCPM. The result suggests that the oxidation due to the addition of NCPM onto the surface sediments made the significant impact on the adsorption of P, the surface sediments had adsorbed a fair amount of P from overlying water because of the addition of external P.

The adsorption data were fitted to the Langmuir isotherm model. The corresponding model parameters are listed in Table 2. Among the five sediments tested, the sediments with the addition of NCPM exhibited the greatest P adsorption, with a higher S_{max} and lower EPC_0 . Compared with the S_{max} and EPC_0 of the control, the S_{max} under the NCPM capping increased by 50.83% (1:1), 68.45% (1:2), 125.68% (1:3) and 171.25% (1:4) and the EPC_0 decreased by 36.44% (1:1), 56.57% (1:2), 76.21% (1:3) and 94.34% (1:4), respectively. The higher S_{max} values and lower EPC_0 values show that the surface sediments were remolded by capping with NCPMs, which has stronger adsorption capacity and immobilization ability. Thus, NCPM could be considered a capping material because of its remediation function on the surface sediments.

3.5. P release from surface sediments under anaerobic conditions

The immobilization of P by the surface sediments (come from the experiment for external P removal and immobilization after 60 days) due to the addition of NCPM were tested by P release from surface sediments under the anaerobic conditions (Fig. 7).

The amount of released P remained at lower levels in the sediments due to the capping with NCPM compared with control. At the first 45 h, the release of P in the control increased sharply to $0.208 \text{ mg (g}\cdot\text{h)}^{-1}$, and was more than that under the capping of NCPM with different ratios (1:1 to 1:4), which ranged from

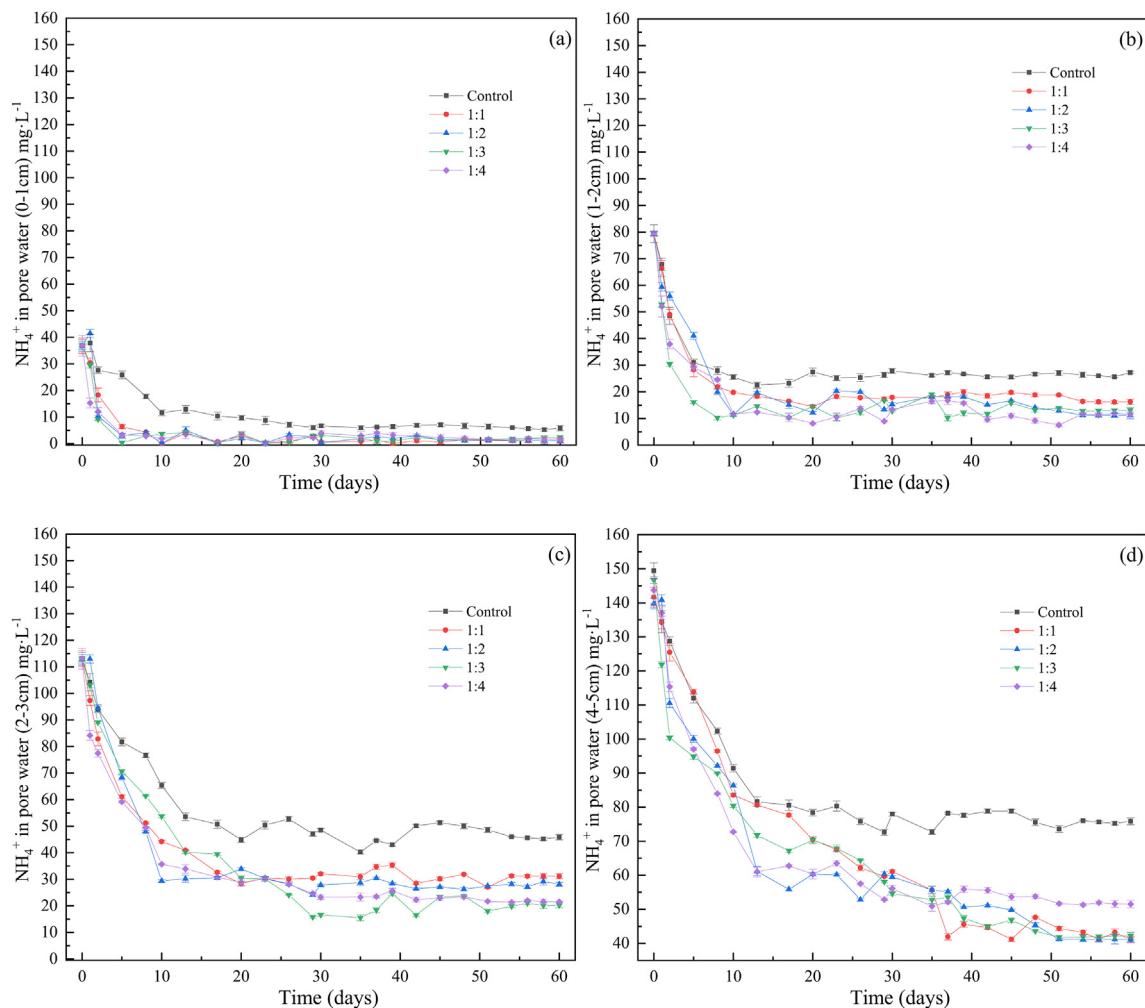


Fig. 4. NH_4^+ concentration of the pore water under the capping with NCPM. Bars indicate SEMs (n = 3).

0.077 mg (g·h) $^{-1}$ to 0.031 mg (g·h) $^{-1}$. The release of P from the surface sediments kept stable until the end of the experiment (P release experiment). Under the capping, the percentages of the total release of P relative to the Tot-P were 0.86% (1:1), 0.59% (1:2), 0.56% (1:3) and 0.39% (1:4), respectively, whereas the value of control was 2.58%. The inhibition of P release from the surface sediments under NCPM was obvious.

4. Discussion

4.1. Properties and P immobilization of surface sediments

4.1.1. The morphological appearance of surface sediments

The morphological appearance of surface sediments was visualized by TEM-EDS (Fig. 8). For the control (Fig. 8a), the surface sediments mainly resembled a loose cluster, whereas, under the NCPM capping with a ratio of 1:4, fibrous clusters were observed. These observations indicate that P coprecipitation formed under the capping with NCPM. It is ascribed to the P adsorption reaction of NCPM in water. Combined with the EDS results, compared with other elements, the percentage of P is similar as Ca, which is 1.98% and 1.91%, respectively. These results are similar to those reported by Yin et al. (2011), who found that suspected Ca–P precipitates onto natural sepiolite after phosphate adsorption.

Fig. 9 shows that the difference in the crystalline phases of

surface sediments after remediation with and without NCPM lies in the formation of calcium carbonate, calcium oxide and hydroxyapatite. For the ratio of 1:1, the sample is mainly composed of calcium carbonate and silica. The diffraction peak at 23°, 29°, 36°, 29°, 43°, 47.5° and 48.5° corresponds to the crystal plane (120), (104), (110), (113), (202), (018) and (118) of calcium carbonate. When the addition amount of NCPM was increased to 1:3 and 1:4, hydroxyapatite formed and its amount increased. With the increase of phosphorus adsorption, the characteristic peak of calcium carbonate decreased significantly, and a new characteristic peak appeared at 25.86° and 31.92° at 2 theta, which was the characteristic peak of calcium phosphate (Guo et al., 2006), indicating that calcium phosphate precipitation was the main form of phosphate removal by this kind of calcium carbonate. Other researcher has observed similar Ca–P precipitates, such as amorphous calcium phosphate (ACP), dicalcium phosphate dihydrate (DCPD) and octacalcium phosphate precipitates (OCP), during P adsorption (Kaasik et al., 2008). These results indicate that surface sediments promote the stable fraction formed after remediation with NCPM.

4.1.2. Langmuir isotherm model

The morphology of surface sediments favors the adsorption and immobilization of P by the surface sediments, as confirmed by the S_{max} and EPC_0 results (Table 2). The result clearly shows that, compared with the S_{max} of the control, the S_{max} of the 1:4 ratio

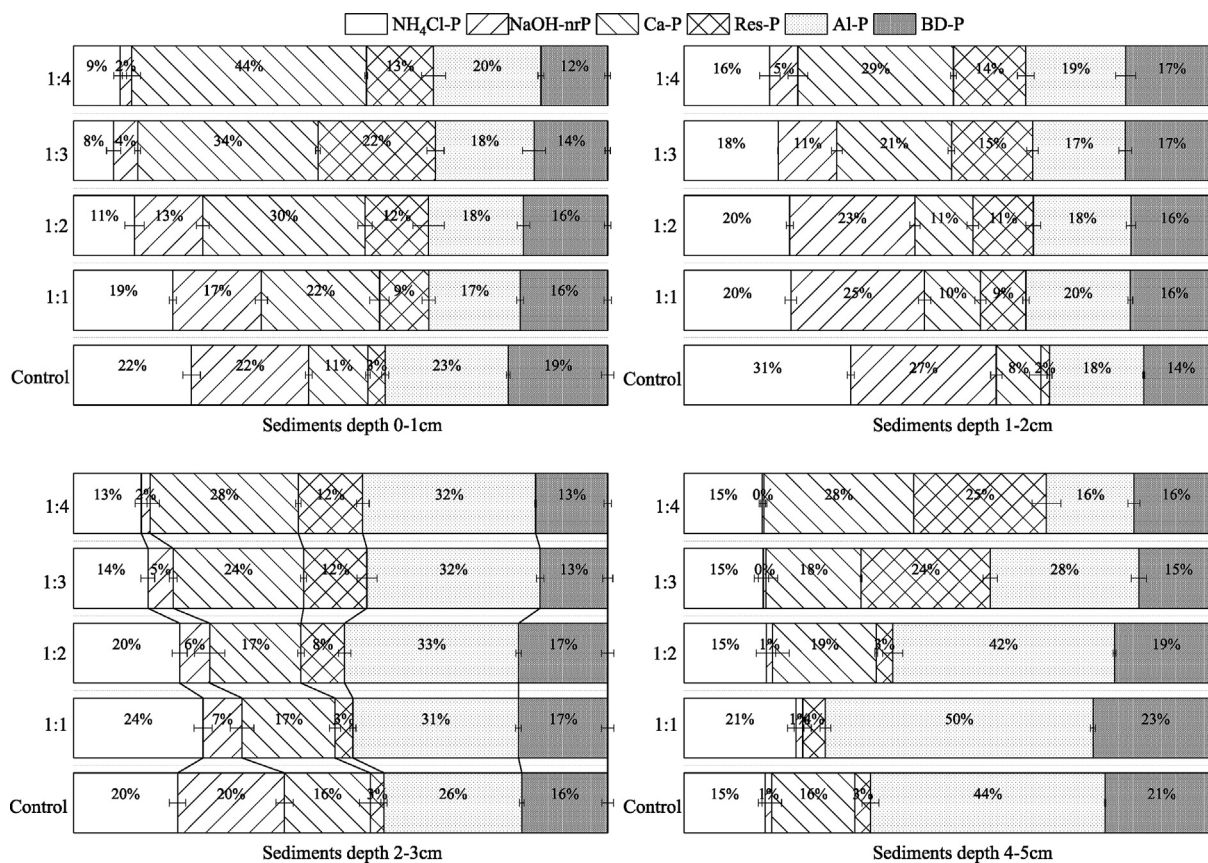


Fig. 5. Sedimentary P fractions under the capping with NCPM. Bars indicate SEMs (n = 3).

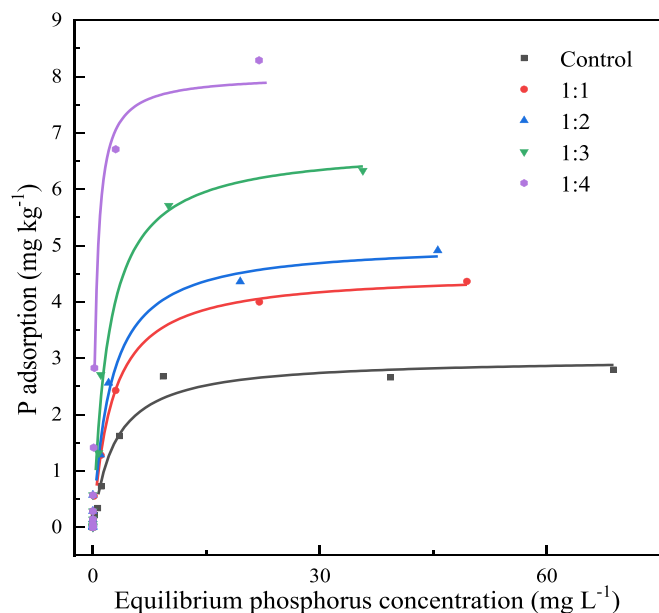


Fig. 6. P adsorption isotherm of different surface sediments after remediation by the NCPM.

increased to as high as 8.143 mg g^{-1} , which indicates that the adsorption capacity on P by the surface sediments was improved because of the capping of NCPM. However, no similar research on the remediation of surface sediments by a capping material has

Table 2

Langmuir parameters for P sorption by surface sediments.

Sediment	$S_{\text{max}}/(\text{mg g}^{-1})$	$n/(\text{L mg}^{-1})$	$\text{EPC}_0/(\text{mg L}^{-1})$	R^2
Control	3.002	0.349	0.601	0.972
1:1	4.528	0.392	0.382	0.989
1:2	5.057	0.428	0.261	0.972
1:3	6.775	0.489	0.143	0.969
1:4	8.143	0.612	0.034	0.986

previously been reported. Therefore, compared with other similar adsorbents. The S_{max} in our study, 6.126 mg g^{-1} (mean for ratios from 1:1 to 1:4, $p < 0.05$), is higher than some values reported by Barca et al. (2012) and Yin et al. (2017) (2.49 mg g^{-1} for EAF-slag and 5.99 mg g^{-1} for 0.2–0.5-mm heated Ca-rich attapulgite). However, it is lower than the values reported for some other adsorbents (89.97 mg g^{-1} for BOF-slag (Bowden et al., 2009) and 42.00 mg g^{-1} for heated Ca-rich attapulgite (Gan et al., 2009)).

The primary reason for the improvement of the adsorption capacity might be the removal of organic matter via oxidation by CaO_2 , resulting in a skeleton with silica and leaving space for the adsorption of P (Wang et al., 2019). Hanh et al. (2005) found that CaO_2 addition enhanced the removal of organic carbon in pond sediment. The organic matter was reported to have decreased from 18% to 4%. An alternative explanation is that metal ions, such as Fe, were transferred from the anaerobic state to the aerobic state (Ding et al., 2018), according to the reduction of Fe (II) in the pore water (Fig. 3).

The surface sediments due to the NCPM not only increases the P adsorption but also improves the sediment remediation and P immobilization, as confirmed by the observed decrease in the EPC_0

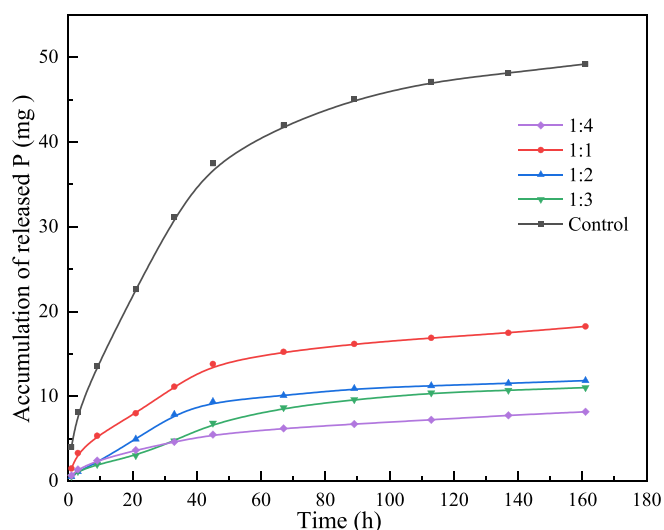


Fig. 7. The accumulation of released P amount in the distilled water under the anaerobic conditions.

(Table 2) which attributed to the transformation of P_{mobile} to inert P. The percentage of the P_{mobile} ($\text{NH}_4\text{Cl-P}$, BD-P and NaOH-nrP) in the surface sediments (0–4 cm) decreased from 57.0% (mean) to 49.9% (mean), 44.4% (mean), 33.3% (mean) and 30.1% (mean) ($P < 0.05$).

The adsorption data were also fitted to the Dubinin-Radushkevich isotherm model (Acemioglu, 2004). The results show that the adsorption energy values for different cases are -8.452 (control), -8.276 (1:1), -8.980 (1:2), -10.541 (1:3) and -11.043 (1:4) $\text{kJ}\cdot\text{mol}^{-1}$, respectively. It is indicating that adsorption of P by surface sediments is mainly by chemical adsorption, ion exchange or chemical precipitation, while the metal ions, such as Ca, Fe and Al, played an important role.

4.1.3. The anaerobic release of sedimentary P

The release of sedimentary P is another indicator used to describe P immobilization in sediments. Compared with the P released from the control, that released from the surface sediments under the capping with NCPM was reduced by 62.92% (1:1), 75.91% (1:2), 77.61% (1:3) and 83.37% (1:4). Additionally, the reduction was enhanced with increasing NCPM dosage. These results indicate that NCPM capping played an important role in inhibiting sedimentary P release, as indicated by the reduction in the P_{mobile} , which ranged from 22.43% (1:2) to 54.71% (1:4), compared with the P_{mobile} at 1:1 ratio. The NaOH-nrP contributes to the largest reduction of P_{mobile} (as much as 87.22% under the ratio of 1:4) compared with the ratio of 1:1. On the contrary, Ca–P remained at a high concentration, as much as 44.00%, suggesting that control of the P release depended on the formation of Ca–P in the sediments.

4.2. Changes of SRP in overlying and pore water

With the external P addition (before day 25), a slighter increase of the SRP in overlying water under NCPM capping with different ratios was observed when compared with the control. When the external P addition was stopped after day 25, the SRP decreased gently (Fig. 1) but the SRP in the control remained at a higher concentration than that under the capping with NCPM. The disappearance of SRP from the overlying water was attributed to chemical precipitation as the main mechanism of P removal by the formation of calcium phosphate minerals under the Ca^{2+} and OH^- via the CaO_2 reaction. The XRD results confirmed this mechanism

(Fig. 9).

Another mechanism is the formation of $\text{Fe}(\text{OOH})\text{-P}$ complexes or precipitates. The reduction of Fe(II) in the pore water verified this (Fig. 3), while the oxidation due to $\cdot\text{OH}$ may be an explanation attributing the reduction of Fe(II) (Kang et al., 2018). The Al and Fe materials in the NCPM, because of the addition of water purification sediments, cannot be excluded as a possible mechanism contributing to the disappearance of SRP. Under oxidation, Fe can be converted into Fe_{ox} (Ding et al., 2018), providing long-term P retention. In addition, the surface sediments after remodeling by the NCPM capping induced a great influence on the removal of P from overlying water, as confirmed by the higher S_{max} and lower EPC_0 values (Table 2).

It is expected that the SRP concentration in pore water decrease as a result of the adsorption and oxidant of NCPM. The results in Fig. 2a, b and 2c confirmed the speculation. However, the results in Fig. 2d contradicted the expected result, showing an increase of the SRP over time and a higher SRP level at sediment depths from 4 to 5 cm compared with those at other sediment depths, such as 0–1 cm (Figs. 2a), 1–2 cm (Fig. 2b) and 2–3 cm (Fig. 2c). These results suggest that the vertical transportation distance of oxygen or $\cdot\text{OH}$ from CaO_2 was not adequate for these species to reach deeper sediments within a short period. The consumption of reducing materials in the sediments on the oxygen or $\cdot\text{OH}$ may be another explanation. The results suggest that the microenvironment at the sediment depths of 4–5 cm is anaerobic or anoxic compared with the microenvironments at the other sediment depths. This hypothesis is confirmed by the higher Fe(II) concentration (Fig. 3d) and higher NH_4^+ concentration (Fig. 4d) at sediment depths from 4 to 5 cm.

The aforementioned experiments show that the P concentrations in the pore water under the capping of the materials that supply oxygen are less than those under the capping of materials that do not supply oxygen (Table 3). By comparison, we found that materials such as Ca, Al and La generally exhibit strong ability to bind P, confirming the significance of the oxic microenvironment in the sediments. In addition, the saturation of P on the capping materials should be improved to deal with the higher P concentration in pore water. Therefore, promoting the conversion of P_{mobile} to inert-P may be a better choice to lengthen the application duration of the capping.

4.3. Sedimentary P fractions and their immobilization

The NCPM, which was used as the capping material, improved the external P precipitation into different P fractions (Fig. 5). In addition, the Tot-P in the sediments (0–4 cm) increased as the ratio was increased from 1:1 to 1:4. This trend might be a consequence of greater oxidation of the surface sediments because the higher ratio of NCPM led to greater adsorption or retention ability on P. Furthermore, the oxidation obviously influenced the redistribution of sedimentary P fractions. Fig. 1 shows that, for the control, the lower external P disappeared from the overlying water, as compared with the capping. We expected the Tot-P of the overlying water in the control to be less than capping. However, the Tot-P in the surface sediments (0–4 cm) in the control was higher than that in the sediments under the capping, suggesting that the disappeared P was mainly incorporated into NCPM, resulting in the lower external P incorporation into the surface sediments.

The capping with NCPM caused a significant decrease of the P_{mobile} in the surface sediments. Compared with the P_{mobile} of the control, that under the NCPM capping was reduced by 17.77% (1:1), 26.26% (1:2), 41.54% (1:3) and 48.87% (1:4) ($P < 0.05$). This reduction in P_{mobile} is attributed to the strong oxidation resulting from the $\cdot\text{OH}$ improving the conversion from a reducing state to an oxic

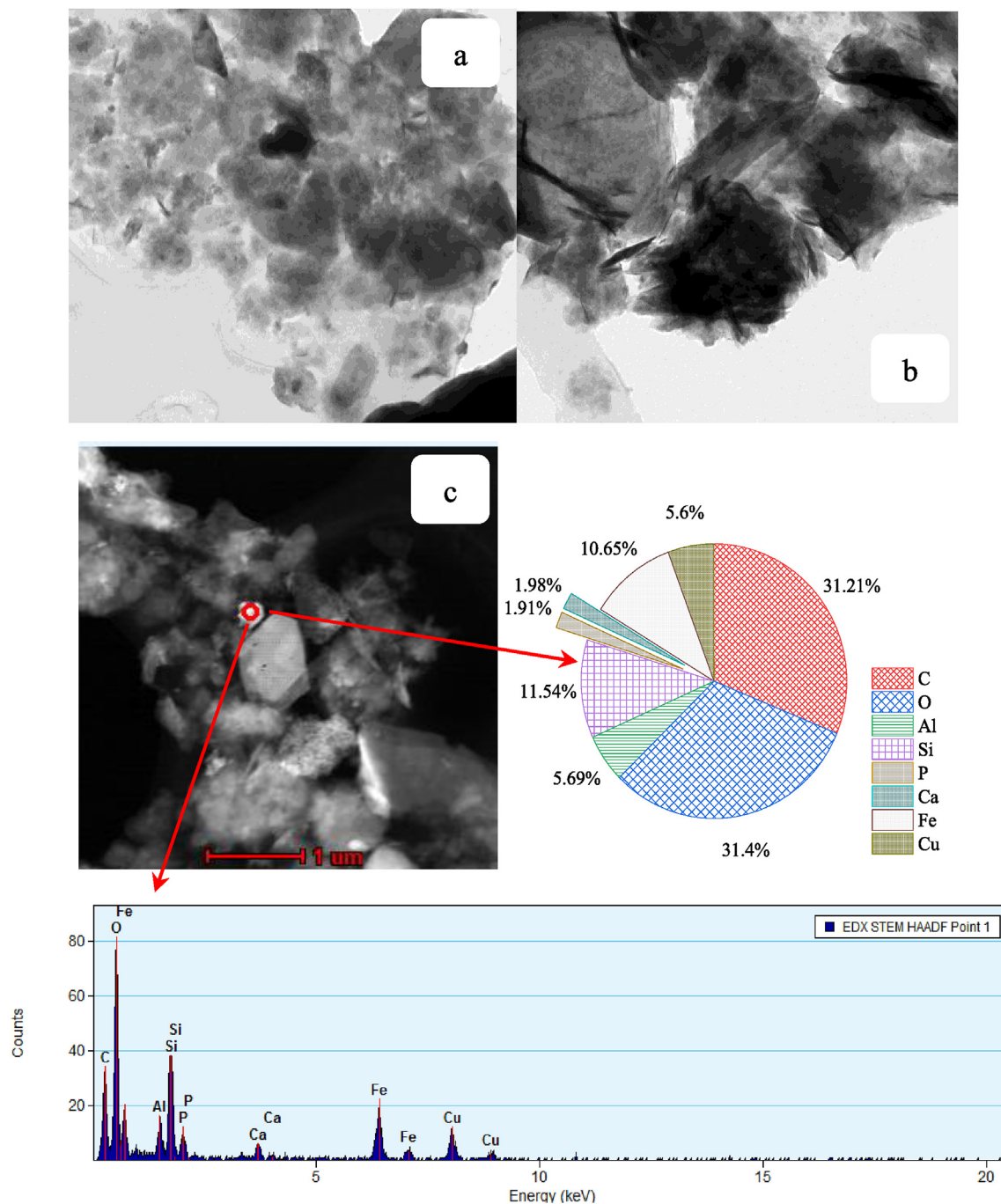


Fig. 8. TEM images and EDS analysis of surface sediment without and with the addition of NCPM. (a) Microstructure of surface sediment without the addition of NCPM. (b) Microstructure of the surface sediment with the addition of NCPM at dosage of 1:4. (c) SEM-EDS analysis spectrum of the surface sediment with the addition of NCPM at dosage of 1:4.

state, such as the conversion of Fe(II) to Fe(III), and resulting in a slighter reduction of BD-P in the surface sediments. The transformation of BD-P from non-occluded to occluded was the main explanation under the oxidation of soluble ferrous (Fe(II)) compounds to insoluble ferric (Fe(III)) compounds. However, for the NaOH-nrP, the reduction ranging from 5.1% (1:1) to 15.28% (1:4) is obviously greater than that for BD-P, which ranged from 0.2% (1:1) to 2.67% (1:4) ($P < 0.05$).

The NaOH-nrP is referred to as organic-P, particularly when P is bound to humic substances, accumulated in microorganisms, or incorporated into organic compounds such as phospholipids (Selig,

2003). Under oxidation by $\cdot\text{OH}$, organic matter becomes more degradable and is removed, resulting in a decrease of the concentration of NaOH-nrP. The conversion of NaOH-nrP to inert P was verified through oxidation in a previous study (Lin et al., 2017). Therefore, reducing the NaOH-nrP promotes a decrease in the mobile sedimentary P fractions and inhibits the algae bloom.

In the case of $\text{NH}_4\text{Cl-P}$, its contribution to the P_{mobile} is the largest. However, under the NCPM capping, the reduction from 1.9% (1:1) to 8.97% (1:4) is greater than that in the case of BD-P ($P < 0.05$). This result indicates that the $\text{NH}_4\text{Cl-P}$ is easily desorbed and competitively adsorbed by other ions such as Fe, Al and

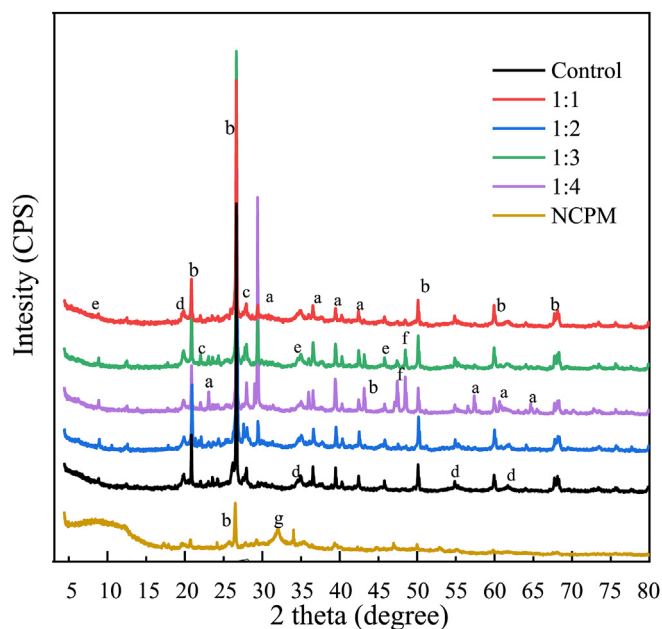


Fig. 9. XRD patterns of surface sediments in different dosages of NCPM (a: Calcite; b: Quartz; c: Albite-calcian ordered; d: Muscovite; e: Gordonite; f: Hydroxyapatite; g: Calcium oxide).

Ca ions.

The reduction of P_{mobile} in the sediments (0–4 cm) was accompanied by a substantial increase of inert-P (the sum of Al–P, Ca–P and Res–P) under the capping, ranging from 50.15% (1:1) to 69.88% (1:4). The contribution of Ca–P to the inert-P is greatest at sediment depths from 0 to 1 cm, primarily because of the penetration of Ca. A previous study (Zhou et al., 2019) about capping with NCPM indicated that the pH in the overlying water can be as high as 8.3, which means that calcium phosphate minerals can precipitate spontaneously. When the pH of overlying water is greater than 8, favourable conditions for the form of Ca–P compounds, including hydroxyapatite and dicalcium phosphate. The reaction of CaO_2 in water can continuously release Ca^{2+} and OH^- to favour P removal (Fig. 1) through the precipitation of calcium phosphate. The mixing of water purification sludge in NCPM smothered the reaction between CaO_2 and water.

Noticeably, at sediment depths from 0 to 1 cm, Ca–P remained at a higher level compared with the Al–P ($P < 0.05$): as high as 44.00% under the ratio of 1:4. Surprisingly, in deeper sediment (2–3 cm and 4–5 cm), Al–P remained at a high concentration compared with the concentration of Ca–P. In this case, Al^{3+} could migrate 5 cm into the sediment, where the Al–P concentration was

41.8%. Other authors have proposed that the strong reactive Ca^{2+} , which has a higher sorption capacity than Al^{3+} , has the capacity to transform Al–P into Ca–P in sediment (0–1 cm) (Lin et al., 2017; Yin et al., 2018). However, the Al^{3+} will permeate into deeper sediments, resulting in a dramatic increase in the amount of Al–P in deeper sediment. Another explanation for the increase of Al–P is that the supply of Al^{3+} from the water purification sludge in the NCPM can support the formation of Al–P.

4.4. Implications of remediation on the surface sediment under the capping

For surface waters, sediments play an important role in remediation because of sedimentary P release. In situ capping to control the sedimentary P release is common. It is obvious that the NCPM can be used the capping materials due to its oxygen and Ca^{2+} supply and its oxidation on the surface sediments.

Notably, the results indicate that the capping with NCPM can not only enhance the removal of P from the overlying water but also improve the sedimentary P immobilization. In addition, the NCPM promotes the remediation of sediments, resulting in a decrease of the concentrations of NH_4^+ and Fe(II) and thereby favouring the reduction of SRP in pore water. This process is attributed to the oxidation by $\cdot\text{OH}$ generated by the reaction of CaO_2 with water. The higher S_{max} and lower EPC_0 of the surface sediments under the capping with NCPM and the addition of external P can verify this. Furthermore, the transformation from P_{mobile} to inert-P in the surface sediments shows sedimentary P immobilization and the reduction of P release. Therefore, the remediation due to the capping with NCPM is also considered as a suitable function mode to control the sedimentary P release.

5. Conclusions

The immobilization on P by the surface sediments due to the capping of NCPM with different ratios (1:1–1:4) was enhanced compared with the control, resulting in P removal amounts as high as 3.97 mg (1:1), 5.15 mg (1:2), 6.97 mg (1:3) and 8.36 mg (1:4). This P removal process is associated with the formation of calcium phosphate minerals and the ability of $\cdot\text{OH}$ to oxidize the surface sediments, resulting in conversion of sedimentary micro-environment conditions from anaerobic to aerobic, which is verified by the reduction of the concentrations of NH_4^+ and Fe(II) in pore water. The higher S_{max} and lower EPC_0 of the surface sediments under the NCPM capping confirmed this. In addition, the removal of SRP from overlying water, the reduction of SRP, NH_4^+ and Fe(II) in pore water, the increase of S_{max} and the decrease of the EPC_0 are closely related to the ratio of NCPM. Furthermore, the P_{mobile} was reduced by 17.77–48.47% and the inert-P increased from 50.15% (1:1) to 69.88% (1:4) under the NCPM capping with different ratios,

Table 3
Reported P concentration in pore water under different capping.

Materials	Dosage (ratio with P_{mobile})	Particle size	Treatment object	P concentration in pore water (mg/L)	Depth under sediment-water interface (mm)	References
NCAP700	25:1	0.2–0.5 mm	Eutrophic lake	0.32–0.50	15–30	Yin and Kong, 2015
Aluminum sulfate	15:1	solution	polluted river	0.12–1.45	20–60	Lin et al. (2017)
lanthanum modified bentonite	200:1	2 mm	freshwater lake	0.17–0.95	20–60	Ding et al. (2018)
TCAP700	200:1	0.5–2 mm	Hypereutrophic lake	0.48	10–30	Yin et al. (2018)
Calcium silicate hydrates	100:1	0.15 mm	Lake water	0.044	No mentioned	Li et al. (2018)
NCPM	4:1	5 mm	Eutrophic lake	0.031–0.112	5–45	This study

compared with the control. It is verified by the release of sedimentary P from surface sediments under anaerobic conditions. The percentage of the released P in the sediments Tot-P was merely 0.60% (mean, from 1:1 to 1:4), which was lower than that in the control (2.58%). The implication of these results is that the remediation due to the capping with NCPM played the important role in controlling the P content in water.

Declaration of competing interest

The authors declare that they have no known competing financial interests or personal relationships that could have appeared to influence the work reported in this paper.

Acknowledgements

This study was supported by the National Natural Science Foundation of China (grant Nos. 51778393), Collaborative Innovation Center of Water Treatment Technology and Material of Jiangsu Province, National and Local Joint Engineering Laboratory of Municipal Sewage Resource Utilization Technology.

References

- Abu-Hmeidan, H., Williams, G., Miller, A., 2018. Characterizing total phosphorus in current and geologic Utah lake sediments: implications for water quality management issues. *Hydrology* 5, 1. <https://doi.org/10.3390/hydrology5010008>.
- Acemioğlu, B., 2004. Adsorption of Congo red from aqueous solution onto calcium-rich fly ash. *J. Colloid Interface Sci.* 274, 371–379. <https://doi.org/10.1016/j.jcis.2004.03.019>.
- Ashley, K.I., Mavinic, D.S., Hall, K.J., 2008. Oxygenation performance of a laboratory-scale Speece Cone hypolimnetic aerator: preliminary assessment. *Can. J. Civ. Eng.* 35 (7), 663–675. <https://doi.org/10.1139/L08-011>.
- Barca, C., Gérente, C., Meyer, D., Chazarenc, F., Andrés, Y., 2012. Phosphate removal from synthetic and real wastewater using steel slags produced in Europe. *Water Res.* 46, 2376–2384. <https://doi.org/10.1016/j.watres.2012.02.012>.
- Bowden, L.L., Jarvis, A.P., Younger, P.L., Johnson, K.L., 2009. Phosphorus removal from waste waters using basic oxygen steel slag. *Environ. Sci. Technol.* 43, 2476–2481. <https://doi.org/10.1021/es801626d>.
- Ding, S.M., Sun, Q., Chen, X., Liu, Q., Wang, D., Lin, J., Zhang, C.S., Tsang, D.C.W., 2018. Synergistic adsorption of phosphorus by iron in lanthanum modified bentonite (Phoslock®): new insight into sediment phosphorus immobilization. *Water Res.* 134, 32–43. <https://doi.org/10.1016/j.watres.2018.01.055>.
- Fox, R., Tuchman, M., 1996. The assessment and remediation of contaminated sediments (ARCS) program. *J. Great Lakes Res.* 22, 493–494. [https://doi.org/10.1016/S0380-1330\(96\)70974-7](https://doi.org/10.1016/S0380-1330(96)70974-7).
- Francingues, K.E.G., Burton, G.A., Wolfe Jr., Reible, D.D., Vorh, D.J., 2008. Evaluating the effectiveness of contaminated-sediment dredging. *Environ. Sci. Technol.* 42, 5042–5047. <https://doi.org/10.1021/es087185a>.
- Gan, B.K., Madsen, I.C., Hockridge, J.G., 2009. In situ X-ray diffraction of the transformation of gibbsite to α -alumina through calcination: effect of particle size and heating rate. *Appl. Crystallogr.* 42, 697–705. <https://doi.org/10.1107/S0021889809021232>.
- Guo, X.H., Yu, S.H., Cai, G.B., 2006. Crystallization in a mixture of solvents by using a crystal modifier: morphology control in the synthesis of highly monodisperse CaCO_3 microspheres. *Angew. Chem.* 118, 4081–4085. <https://doi.org/10.1002/ange.200600029>.
- Hanh, D.N., Rajbhandari, B.K., Annachatre, A.P., 2005. Bioremediation of sediments from intensive aquaculture shrimp farms by using calcium peroxide as slow oxygen release agent. *Environ. Technol.* 26, 581–589. <https://doi.org/10.1080/09593332608618543>.
- Huang, X., Dong, W.Y., Wang, H.J., Sun, F.Y., Feng, Y.Y., 2019. Enhance primary sludge acidogenic fermentation with CaO_2 addition: investigation on soluble substrate generation, sludge dewaterability, and molecular biological characteristics. *J. Clean. Prod.* 228, 1526–1536. <https://doi.org/10.1016/j.jclepro.2019.04.361>.
- Jin, X.C., Wang, S.R., Pang, Y., Zhao, H.C., Zhou, X.N., 2005. The adsorption of phosphate on different trophic lake sediments. *Colloids Surf., A* 254, 241–248. <https://doi.org/10.1016/j.colsurfa.2004.11.016>.
- Kaasik, A., Vohla, C., Mötelp, R., Mander, U., Kirsimäe, K., 2008. Hydrated calcareous oil-shale ash as potential filter media for phosphorus removal in constructed wetlands. *Water Res.* 42, 1315–1323. <https://doi.org/10.1016/j.watres.2007.10.002>.
- Kang, M.X., Peng, S., Tian, Y.M., Zhang, H.Y., 2018. Effects of dissolved oxygen and nutrient loading on phosphorus fluxes at the sediment–water interface in the Hai River Estuary, China. *Mar. Pollut. Bull.* 130, 132–139. <https://doi.org/10.1016/j.marpolbul.2018.03.029>.
- Li, C.J., Yu, H.X., Tabassum, S., Li, L.F., Wu, D.Y., Zhang, Z.J., Kong, H.N., Pei, X., 2017. Effect of calcium silicate hydrates (CSH) on phosphorus immobilization and speciation in shallow lake sediment. *Chem. Eng. J.* 317, 844–853. <https://doi.org/10.1016/j.cej.2017.02.117>.
- Li, C.J., Yu, H.X., Tabassum, S., Li, L.F., Mu, Y.L., Wu, D.Y., Zhang, Z.J., Kong, H.N., Xu, P., 2018. Effect of calcium silicate hydrates coupled with *Myriophyllum Spicatum*, on phosphorus release and immobilization in shallow lake sediment. *Chem. Eng. J.* 331, 462–470. <https://doi.org/10.1016/j.cej.2017.08.134>.
- Lin, J., Sun, Q., Ding, S., Wang, D., Wang, Y., Chen, M., Shi, L., Fan, X., Tsang, D.C.W., 2017. Mobile phosphorus stratification in sediments by aluminum immobilization. *Chemosphere* 186, 644–651. <https://doi.org/10.1016/j.chemosphere.2017.08.005>.
- Meis, S., Spears, B.M., Maberly, S.C., O'Malley, M.B., Perkins, R.G., 2012. Sediment amendment with Phoslock? in Clatto Reservoir (Dundee, UK): investigating changes in sediment elemental composition and phosphorus fractionation. *J. Environ. Manag.* 93, 185–193. <https://doi.org/10.1016/j.jenvman.2011.09.015>.
- Meis, S., Spears, B.M., Maberly, S.C., Perkins, R.G., 2013. Assessing the mode of action of Phoslock? in the control of phosphorus release from the bed sediments in a shallow lake (Loch Flemington, UK). *Water Res.* 47, 4460–4473. <https://doi.org/10.1016/j.watres.2013.05.017>.
- Müller, R., Stadelmann, P., 2010. Fish habitat requirements as the basis for rehabilitation of eutrophic lakes by oxygenation. *Fish. Manag. Ecol.* 11, 251–260. <https://doi.org/10.1111/j.1365-2400.2004.00393.x>.
- Pan, G., Dai, L., Li, L., He, L., Li, H., Bi, L., Gulati, R.D., 2012. Reducing the recruitment of sedimented algae and nutrient release into the overlying water using modified soil/sand flocculation-capping in eutrophic lakes. *Fish. Manag. Ecol.* 46, 5077–5084. <https://doi.org/10.1021/es3000307>.
- Rydin, E., 2000. Potentially mobile phosphorus in lake erlen sediment. *Water Res.* 34, 2037–2042. [https://doi.org/10.1016/S0043-1354\(99\)00375-9](https://doi.org/10.1016/S0043-1354(99)00375-9).
- Selig, U., 2003. Particle size-related phosphate binding and P-release at the sediment–water interface in a shallow German lake. *Hydrobiologia* 492, 107–118. <https://doi.org/10.1016/j.cej.2017.08.134>.
- Sibrell, P.L., Montgomery, G.A., Ritenour, K.L., Tucker, T.W., 2009. Removal of phosphorus from agricultural wastewaters using adsorption media prepared from acid mine drainage sludge. *Water Res.* 43, 2240–2250. <https://doi.org/10.1016/j.watres.2009.02.010>.
- State Environmental Protection Administration (SEPA) of China, 2002. *Monitor and Analysis Method of Water and Wastewater*. Chinese Environmental Science Publication House, Beijing.
- Stow, C.A., Cha, Y.K., 2013. Are chlorophyll a-total phosphorus correlations useful for inference and prediction? *Environ. Sci. Technol.* 47, 3768–3773. <https://doi.org/10.1021/es304997p>.
- Wang, L., Chen, S.S., Sun, Y.Q., Tsang, D.C.W., Yip, A.C.K., Ding, S.M., Hou, D.Y., Baek, K., Ok, Y.S., 2018a. Efficacy and limitations of low-cost adsorbents for in-situ stabilization of contaminated marine sediment. *J. Clean. Prod.* 212, 420–427. <https://doi.org/10.1016/j.jclepro.2018.12.056>.
- Wang, S.D., Kong, L.J., Long, J.Y., Su, M.H., Diao, Z.H., Chang, X.Y., Chen, D.Y., Song, G., Kaimin, S., 2018b. Adsorption of phosphorus by calcium-flour biochar: isotherm, kinetic and transformation studies. *Chemosphere* 195, 666–672. <https://doi.org/10.1016/j.chemosphere.2017.12.101>.
- Wang, Z., Lu, S.Y., Wu, D.Y., Chen, F.X., 2017. Control of internal phosphorus loading in eutrophic lakes using lanthanum-modified zeolite. *Chem. Eng. J.* 327, 505–513. <https://doi.org/10.1016/j.cej.2017.06.111>.
- Wang, W.H., Wang, Y., Fan, P., Chen, L.F., Chai, B.H., Zhao, J.C., Sun, L.Q., 2019. Effect of calcium peroxide on the water quality and bacterium community of sediment in black-odor water. *Environ. Pollut.* 248, 18–27. <https://doi.org/10.1016/j.envpol.2018.11.069>.
- Yamada-Ferraz, T.M., Sueitt, A.P.E., Oliveira, A.F., Botta, C.M.R., Fadini, P.S., Nascimento, M.R.L., Faria, B.M., Mozeto, A.A., 2015. Assessment of Phoslock® application in a tropical eutrophic reservoir: an integrated evaluation from laboratory to field experiments. *Environ. Technol. Innov.* 4, 194–205. <https://doi.org/10.1016/j.eti.2015.07.002>.
- Yin, H.B., Kong, M., 2015. Reduction of sediment internal P-loading from eutrophic lakes using thermally modified calcium-rich attapulgite-based thin-layer cap. *J. Environ. Manag.* 151, 178–185. <https://doi.org/10.1016/j.jenvman.2015.01.003>.
- Yin, H.B., Yun, Y., Zhang, Y.L., Fan, C.X., 2011. Phosphate removal from wastewaters by a naturally occurring, calcium-rich sepiolite. *J. Environ. Manag.* 198, 362–369. <https://doi.org/10.1016/j.jhazmat.2011.10.072>.
- Yin, H.B., Yan, X.W., Gu, X.H., 2017. Evaluation of the thermally-modified calcium-rich attapulgite as a lowcost substrate for rapid phosphorus removal in constructed wetlands. *Water Res.* 115, 329–338. <https://doi.org/10.1016/j.watres.2017.03.014>.
- Yin, H.B., Douglas, G.B., Cai, Y.J., Liu, C., Copetti, D., 2018. Remediation of internal phosphorus loads with modified clays, influence of fluvial suspended particulate matter and response of the benthic macroinvertebrate community. *Sci. Total Environ.* 610–611, 101–110. <https://doi.org/10.1016/j.scitotenv.2017.07.243>.
- Yu, J.H., Ding, S.M., Zhong, J.C., Fan, C.X., Chen, Q.W., Yin, H.B., Zhang, L., Zhang, Y.L., 2017. Evaluation of simulated dredging to control internal phosphorus release from sediments: focused on phosphorus transfer and resupply across the sediment–water interface. *Sci. Total Environ.* 592, 662–673. <https://doi.org/10.1016/j.scitotenv.2017.02.219>.
- Zhou, J., Li, D.P., Chen, S.T., Xu, Y., Geng, X., Guo, C.R., Huang, Y., 2019. Sedimentary phosphorus immobilization with the addition of amended calcium peroxide material. *Chem. Eng. J.* 357, 288–297. <https://doi.org/10.1016/j.cej.2018.09.175>.